Journal of Sol-Gel Science and Technology 34, 173–179, 2005
© 2005 Springer Science + Business Media, Inc. Manufactured in The Netherlands.

Effect of Fluorine Doping on Semiconductor to Metal-Like Transition and Optical Properties of Cadmium Oxide Thin Films Deposited by Sol–Gel Process

P.K. GHOSH, S. DAS, S. KUNDOO AND K.K. CHATTOPADHYAY*
Department of Physics, Jadavpur University, Kolkata - 700 032, India
kkc@juphys.ernet.in

Received May 19, 2004; Accepted January 27, 2005

Abstract. Highly conducting fluorine doped n-type cadmium oxide thin films have been synthesized by sol–gel dip coating process on glass and Si substrates for various fluorine concentrations in the films. X-ray diffraction pattern confirmed the cubic CdO phase formation and SEM micrograph showed fine particles of CdO with size $\sim$0.3 μm. F concentration in the films was varied from 1.8% to 18.7% as determined from energy dispersive X-ray analysis (EDX). The resistivity of the CdO films decreased with increase of F doping and increase of temperature below 14.6% of F, as usual for semiconductors. Above this F concentration the resistivity increased with increase of temperature like metals. Hall measurement showed very high carrier concentrations in the films lying in the range of $\sim 2.93 \times 10^{20}$ cm^{-3} to 4.56×10^{21} cm^{-3}. UV-VIS-NIR spectrum of the films showed the optical bandgap energy increased with increase of F doping and corresponding carrier concentrations obtained from Burstein-Moss shift also support the Hall measurement results.

Keywords: cadmium oxide, fluorine doping, phase transition, Burstein-Moss shift

1. Introduction

Highly conducting transparent semiconductors, that can be grown efficiently as thin films with low cost, are used extensively for a variety of applications including architectural windows, thin film photo-voltaic and many other opto-electronic devices [1, 2]. n-type transparent conducting oxides (TCOs), such as tin oxide (SnO_2) [3], zinc oxide (ZnO) [4], indium tin oxide (ITO) [5], cadmium oxide (CdO) [6–8], cadmium stannate (Cd_2SnO_4) [9] etc. and p-type such as $CuAlO_2$ [10, 11], $CuScO_{2+x}$ [12], $SrCu_2O_2$ [13] etc. have great technological interest due to their electrical and optical properties. Electrically high conducting and optically transparent materials, like tin oxide and cadmium oxide may also be utilized as windshield defrosting layer for airplanes [14].

Studies of the electrical and optical properties of CdO thin films synthesized by various techniques, including activated reactive evaporation [6], solution growth [7], spray pyrolysis [15, 16], rf sputtering [17], MOCVD [8], PLD [18] etc. have been reported. CdO single crystals have been grown by metalorganic molecular-beam epitaxy [19] and vapor phase reaction [20]. Though polycrystalline CdO thin films are not a popular TCO material due to the narrow optical band gap, it has demonstrated higher electron mobility than that of other TCOs. Having low electrical resistivity, high electron mobilities and low visible absorption, CdO has been suitable for a wide range of applications. Previous work on CdO [21] has proven that CdO always contains excess Cd, and point defects are created due to either Cd interstitials or oxygen vacancies, which act as doubly charged doners. Electrical measurements on CdO single crystals showed n-type conductivity in the range of $\sim 10^2$ to 10^3 S/cm.

*To whom all correspondence should be addressed.

Doping of CdO thin films with various elements like In by Freeman et al. [8], Sn by Yan et al. [18] and F by Ghosh et al. [22] have been done to increase the conductivity. The maximum conductivity was reported as $\sim 4.2 \times 10^4$ S/cm for Sn-doped epitaxially grown CdO films by Yan et al. [18] and 1.08×10^4 S/cm for sol–gel derived F-doped CdO thin films by Ghosh et al. [22]. For decreasing the resistivity of an n-type semiconducting material, the non-metal doping is more efficient than metal doping. Fluorine has been used as a suitable dopant for other transparent conducting thin films like ZnO [23]. We have recently reported properties of fluorine doped SnO_2 [24] and fluorine doped CdO thin films deposited by sol–gel process. Fluorine has seven electrons in the last orbit and oxygen has six, hence F doping increases excess electrons in CdO and thereby increases the n-type conductivity. Detail study on the temperature variation of electrical resistivity with percent of doping indicated a semiconductor to metal-like transition for such films. Also variation of optical bandgap with doping concentration was observed. A literature survey shows that such semiconductor to metal-like transition has not been reported for CdO films so far. In this paper we report the effect of F doping on semiconductor to metal-like phase transition and optical properties of CdO thin films deposited by the sol–gel process.

2. Experimental Details

2.1. Synthesis

The films were deposited on glass and Si substrates using sol–gel dip coating process. Different solutions were prepared by mixing cadmium acetate (99.99% $Cd(COOCH_3)_2$) and ammonium fluoride (99.95% NH_4F) with different atomic ratios of Cd:F, dissolved in a mixture of isopropyl alcohol and double distilled water (2:1). The pH of the solution was controlled at $\sim$5 by adding appropriate amounts of acetic acid (99.95% CH_3COOH). The solution was stirred by a magnetic stirrer and heated at a constant temperature of $\sim 80^\circ$C for a one hour. The solution was aged for two hours. Before dip coating the glass substrates were cleaned by mild soap solution, washed thoroughly by distilled water and then in boiled water. Finally it was degreased in alcohol vapor. Si substrates were cleaned at first in 20% HF solution for 5 min and then washed in acetone in an ultrasonic cleaner. The cleaned substrates were dipped vertically into the solution and withdrawn very slowly at a speed of $\sim$8 cm/min and dried at 100°C for 15 min for quick gel formation. This process was repeated for six to seven times. Finally the coated substrate was heated at 400°C for two hours in open air; the films suddenly turn into a yellow-brown color due to the formation of CdO.

In case of the sol–gel synthesis of CdO, the formation of inorganic polymerization (—Cd—O—Cd—) may be represented as follows [14]:

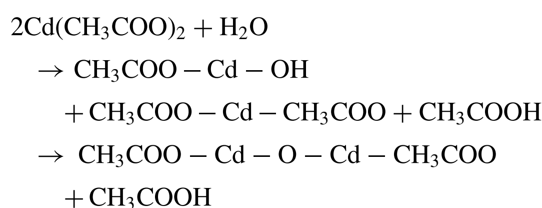

$$
\begin{aligned}
&2Cd(CH_3COO)_2 + H_2O \\
&\quad \rightarrow CH_3COO - Cd - OH \\
&\qquad + CH_3COO - Cd - CH_3COO + CH_3COOH \\
&\quad \rightarrow CH_3COO - Cd - O - Cd - CH_3COO \\
&\qquad + CH_3COOH
\end{aligned}
$$

During annealing at high temperature (400°C), water and carbon groups are removed. The overall generalized reaction can be written as:

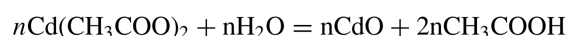

$$nCd(CH_3COO)_2 + nH_2O = nCdO + 2nCH_3COOH$$

2.2. Characterization

After the films were deposited, they were characterized by different techniques. Structural characterization was done by studying X-ray diffraction (XRD, Bruker D-8 Advance), Fourier transform infrared spectroscopy (FTIR, Nicolet Magna-750) and scanning electron microscopy (SEM, JEOL-5200). Compositional analysis was done by energy dispersive X-ray analysis (EDX, LEICA S-440 Oxford-ISIS). The optical studies were performed by measuring transmittance in the wavelength range $\lambda = 300$–1500 nm using a UV-VIS-NIR spectrophotometer (Hitachi U3410). The electrical conductivity was measured by usual four-probe technique using Keithley electrometer (model 6514) to measure the current. The values of carrier concentration, mobility and type of the carrier were determined from Hall effect studies. Also thermoelectric power measurements confirmed that the material was n-type.

3. Results and Discussion

3.1. Structural Characterization

X-ray diffraction pattern of a representative CdO:F film using Cu K_α radiation ($\lambda = 1.5406$ Å) is shown in

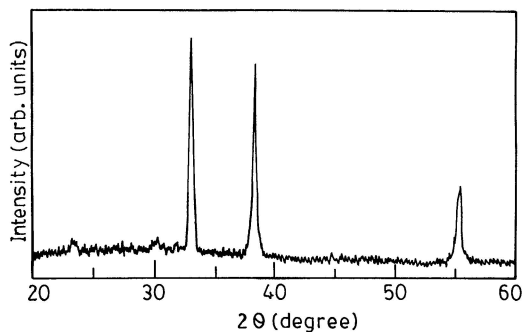

Figure 1. XRD spectra of F:CdO thin film deposited on glass substrate.

Fig. 1. Three peaks are appear due to diffraction from (111), (200) and (220) planes of face centered cubic CdO with $a_0 = 4.6953$ Å [25].

Figure 2 shows the FTIR spectrum of a CdO:F film deposited on a Si substrate. The bands have been assigned to the absorption peaks due to Cd—O, Cd—F and Si—O bond vibrations. The peaks in the range of 460 cm^{-1} to 510 cm^{-1} were assigned to Cd—O bond vibrations in CdO:F and a small peak at 1078 cm^{-1} was attributed to Si—O bond vibration [22]. The peak of Si—O bond vibration has occurred in the spectrum due to the use of the Si substrate, which may be oxidized at the surface because of air annealing of the film at 673 K.

Figure 3 shows the SEM micrograph of a representative CdO:F film deposited on glass substrate for magnification 3500. The micrograph clearly indicated the existence of grains, the average grain size of which was

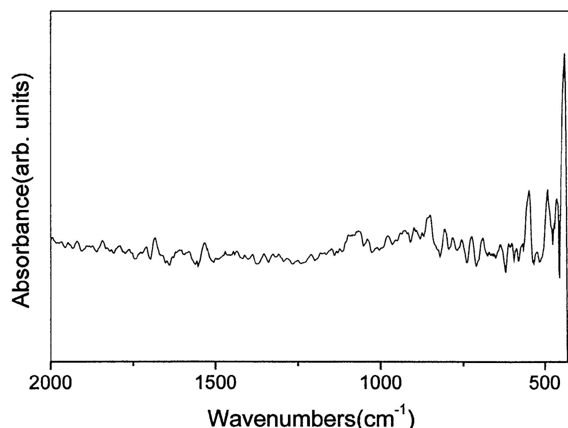

Figure 2. FTIR spectrum of F:CdO thin film deposited on Si substrate.

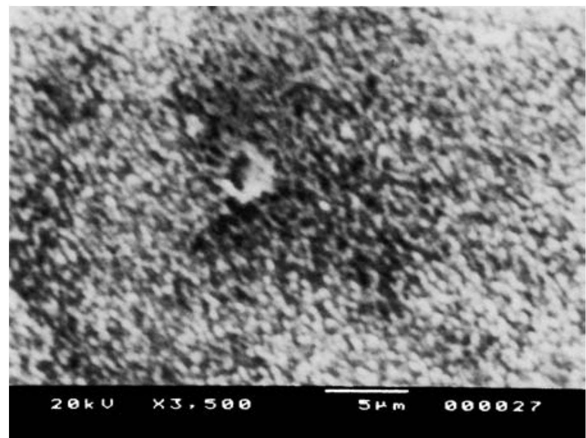

Figure 3. SEM micrograph of F:CdO thin film deposited on glass substrate.

found to be ~0.3 μm. The grains might be composed of smaller crystallites. From a cross sectional SEM measurement (not shown here) the thickness of the films was measured to be ~1.2 μm.

3.2. Compositional Analysis

The final fluorine content in the films was determined by energy dispersive X-ray analysis (EDX). It was seen that, the F/Cd atomic ratio inside the film was lower than that taken in the starting solution. For obtaining minimum resistivity in the deposited films, the presence of high concentration of F ions in the starting solution was required. From Hall measurements and optical (Burstein-Moss shift) studies, charge carrier concentrations in the films with different fluorine content were determined. It was found that, the amount of fluorine atoms acting as a donor, as calculated from Hall effect and Burstein-Moss shift studies, were lower than that of the EDX results. This means that there was an excess of fluorine, incorporated in interstitial positions and in grain boundary regions. The percentage of fluorine doping as obtained from EDX measurement and carrier concentrations obtained from both Hall measurements and Burstein-Moss shift studies are shown in Table 1.

3.3. Electrical Properties

For semiconductor materials, doping in them often induces dramatic changes in their electrical and optical

Table 1. The percentage of fluorine (%F) doping obtained from EDX measurement and carrier concentrations obtained from Hall measurements (n_{Hall}) and Burstein-Moss shift (n_{Optical}) studies.

Sample name	% F from EDX	n_{Hall} (cm^{-3})	n_{Optical} (cm^{-3})
cf-13	1.8	–	–
cf-32	5.6	4.15×10^{20}	2.13×10^{20}
cf-37	8.6	9.64×10^{20}	3.33×10^{20}
cf-29	10.3	1.92×10^{21}	5.63×10^{20}
cf-46	12.8	2.53×10^{21}	9.42×10^{20}
cf-45	14.6	3.3×10^{21}	1.106×10^{20}
cf-47	18.7	4.56×10^{21}	1.279×10^{21}

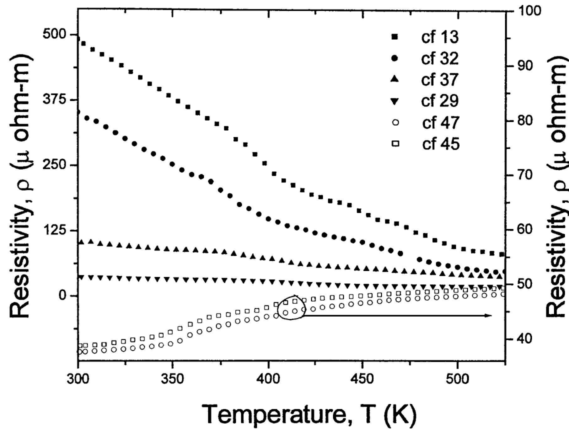

Figure 4. Plots of resistivity (ρ) vs. temperature (T) for different F concentrations.

properties and may alter the bandgap. The electrical resistivity (ρ) of the films deposited with different concentrations of fluorine has been measured at temperature (T) ranging from 300 to 550 K. Plots of resistivity (ρ) vs. temperature (T) for different F concentrations are shown in Fig. 4. The resistivity decreases with increase of temperature below 14.6% of fluorine concentration, as usually observed in a semiconductor. For further increase of fluorine concentration, the reversed phenomena of temperature dependence on resistivity is observed, i.e resistivity increases with increase of temperature due to scattering of charge carriers, just like a metal. Ito et al [26] had also obtained the same type of phase transition phenomena in their Zr doped β-$FeSi_2$ thin film.

The Hall-Effect of the films for different F concentrations has also been studied at room temperature (300 K). From the measured values of Hall coefficient (R_H), we have calculated carrier concentrations (n) for different % F doped CdO thin films using the relation $R_H = -1/\text{ne}$, where e is the electronic charge. The carrier concentrations obtained from Hall measurements are very high $\sim 10^{21}$ cm^{-3}, almost metallic. The mobility (μ) of the carriers was also calculated from the simple relation $\mu = R_H/\rho$.

From the electrical resistivity and Hall measurements data it is evident that the increase of %F doping causes an increase in carrier concentration. This occurs because F atoms can replace O atoms and donate extra electrons to the charge carriers. At first when percentage of doping is small, the rate of increase of carrier concentration is high and it is lower when percentage of doping is high. This phenomenon suggests that the F dopants are not readily ionized and some of them act as neutral impurities in the CdO thin films.

The Hall mobility of the films first increases with additional doping, reaching a maximum value and then decreases for higher % F doping. The simultaneous increase of both mobility and carrier concentration is difficult to explain from the point of view of ionized impurity scattering only, and thus here grain boundary scattering must also be taken into account. Apparently, there exists competition between different scattering mechanisms, which control the Hall mobility. Firstly, the increase of doping lowers the potential barrier height at grain boundaries [27], so the charge carriers can easily cross the grain boundaries. This increases the carrier mobility. Secondly, additional doping can cause the formation of more larger angle grain boundaries. The increase of large angle grain boundaries and both ionized and neutral impurity centers will increase charge carrier scattering, which results in decrease of carrier mobility. Since the scattering probability is inversely proportional to the relaxation time and therefore to mobility, the mobilities due to various scattering mechanisms add inversely

$$1/\mu = 1/\mu_L + 1/\mu_I + 1/\mu_G \quad (1)$$

Increase of carrier concentration can be achieved by increased doping. However, it lowers the mobility due to more charge carrier scattering from ionized impurities. The main scattering mechanisms for charge carriers in thin films are lattice scattering, ionized impurity scattering and grain boundary scattering [18]. The lattice scattering mobility, μ_L, is proportional to the reciprocal of temperature [18], i.e., $\mu_L \propto 1/T$.

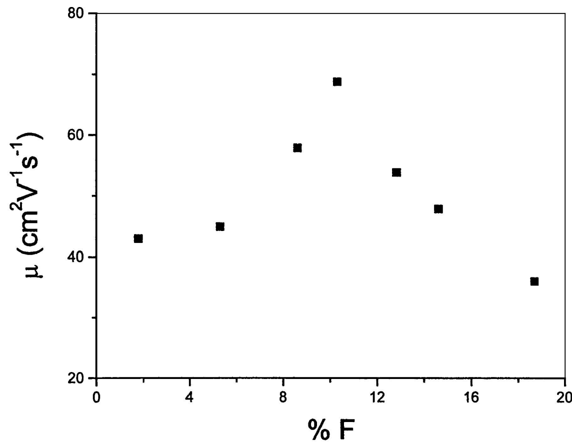

Figure 5. Variation of Hall-mobility with percentage of fluorine doping.

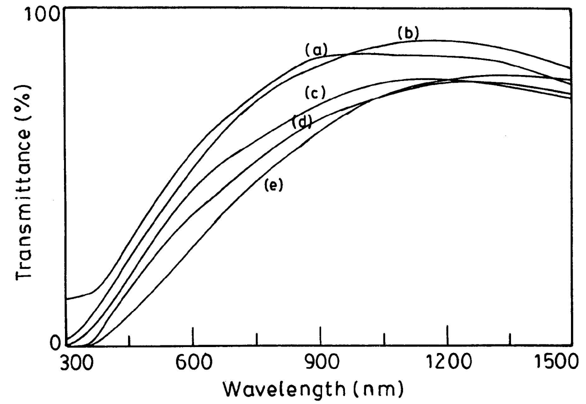

Figure 6. Transmission spectra of F:CdO thin films for five different F concentrations in the films (a) cf-47,18.7% F; (b) cf-45,14.6% F; (c) cf-46, 12.8% F; (d) cf-29, 10.3% F and (e) cf-32,5.6% F.

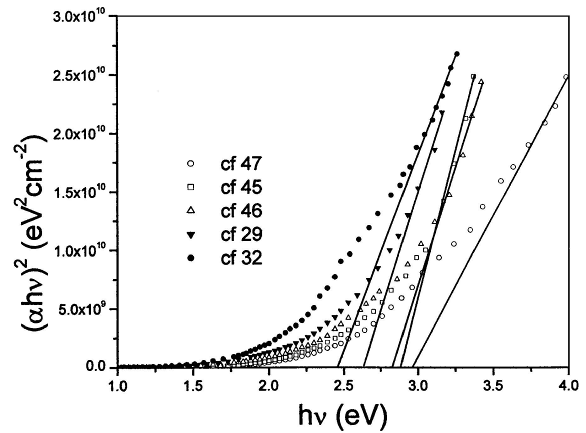

Figure 7. To determine the optical bandgap from $(\alpha h\nu)^2$ vs. $h\nu$ plot.

Ionized impurity scattering mobility, μ_I, is independent of T and decreases with increase of carrier concentration. There are different opinions about the role of grain boundary scattering μ_G. According to Shanthi [28] and Pisarkiewcz [29] the grain boundary scattering was important in limiting the mobility of their films, while others [27, 30] concluded that it made a very small contribution to the mobility behavior.

Figure 5 shows the variation of Hall-mobility with percentage of fluorine doping. It is clear from this figure that the mobility increases with increase of fluorine doping, and reaches a maximum value and then with a further increase of fluorine doping, it decreases due to lattice scattering.

3.4. *Optical Studies*

The optical band gap of fluorine doped cadmium oxide thin films have been determined at 300 K from the transmittance (T) vs. wavelength (λ) plot shown in Fig. 6 for different percentage of F doping. The fundamental absorption, which corresponds to electron excitation from the valance band to conduction band, can be used to determine the nature and value of the optical band gap. The relation between the absorption coefficient (α) and the incident photon energy *($h\nu$)* can be written as [31],

$$(\alpha h\nu)^{1/n} = A(h\nu - E_g) \quad (2)$$

where A is a constant and E_g is the band gap of the material and exponent n depends on the type of transition. $n = 1/2$, 2, 3/2 and 3 corresponding to allowed direct, allowed indirect, forbidden direct and forbidden indirect transitions respectively. Taking $n = 1/2$. $(\alpha h\nu)^2$ vs. $h\nu$ graph (Fig. 7) was plotted and extrapolating the linear portion of the graph to the $h\nu$ axis allowed the direct band gap to be determined from the intercept. The values of the optical bandgap (E_{opt}) lie in the range 2.43 to 2.96 eV.

It may be noted that for higher fluorine doping, the lower is the resistivity and the optical band edge shifts towards lower wavelengths. The shift of optical bandgap from that of the intrinsic bandgap (E_g) of CdO is utilized to calculate the carrier concentrations by using the following relation [32]:

$$E_{\text{opt}} = E_g + (h^2 n^{2/3})/8m_e^* \pi^{2/3} \quad (3)$$

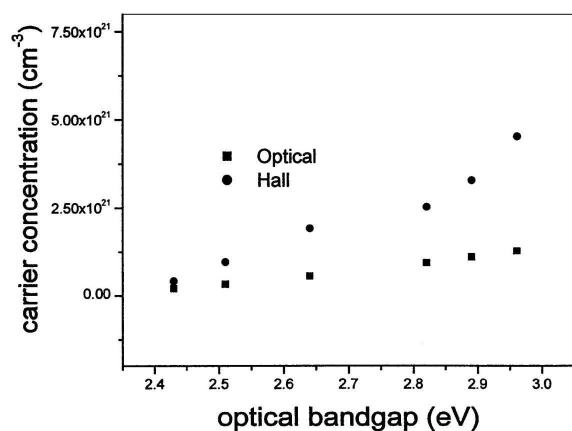

Figure 8. Variation of carrier concentrations obtained from Hall measurement and Burstein- Moss shift with optical bandgap.

where h is the Plank constant, $m_e^* = 0.274$ m$_0$ is the effective mass of electrons in CdO thin films [33]. $E_g = 2.22$ eV is the intrinsic bandgap of CdO thin films, E_{opt} is the optical bandgap obtained from transmittance data and n is the carrier concentration. The carrier concentrations obtained from the above relation lie in the range 2.13×10^{20} cm^{-3} to 1.28×10^{21} cm^{-3} which are marginally less than those obtained from Hall measurements. This may be due to change of carrier concentration effective-mass changes as reported by Coutts et al. [33] in their report on CdO where effective mass increases with increase of carrier concentration, and Young et al. [34] also reported that the effective-mass of electrons in ZnO changes from 0.3 m$_0$ to 0.45 m$_0$ for an order of magnitude increase of carrier concentration. So in our case carrier concentrations obtained from the Burstein-Moss shift at lower F concentrations match fairly well with those obtained from Hall measurements, but at higher F doping, may be due to an increase of effective-mass which is not considered in our calculation. These carrier concentrations are slightly less than actual carrier concentration obtained from Hall measurements. The plot of variation of optical bandgap with carrier concentrations obtained from Burstein-Moss shift and Hall measurement are shown in Fig. 8.

4. Conclusions

Thin films of F doped CdO have been grown by the sol–gel process for different concentrations of F. All the scattering mechanisms of ionized impurity, grain boundary and lattice scattering influenced the mobility behavior of CdO thin films. The increase of doping increased the carrier concentration and hence increased the electrical conductivity. The carrier concentrations obtained from Hall measurements of the films varied from 2.93×10^{20} cm^{-3} to 4.56×10^{21} cm^{-3} and the corresponding optical bandgaps varied from 2.43 to 2.96 eV. The carrier concentrations obtained from Burstein-Moss shift lie within 2.13×10^{20} cm^{-3} to 1.279×10^{21} cm^{-3} which are very high, almost metal-like, and generally support the Hall measurement results. The electrical resistivity decreases with increase of temperature below 14.6% of F doping, and above it resistivity increases with increase of temperature like a metallic behavior. Highly conducting transparent CdO thin films may find many applications such as a low resistance contact to the junction, gas sensors etc. Metallic CdO coating onto glass container may also reduce appreciably the coefficient of friction of the glass surfaces and thereby facilitate the movement of the containers through high-speed fitting lines. Apart from these, highly conducting CdO coating may be used for the production of heating layers for protecting vehicle windscreens from freezing and misting over; light transmitting electrodes for development of optoelectronic devices; antistatic surface layers on temperature control coatings in orbiting satellites and surface layers in electroluminescent applications.

Acknowledgment

One of us (SD) wishes to thank University Grants Commission (UGC), Govt. of India, for awarding him a junior research fellowship (JRF) during the execution of the work.

References

1. D.S. Ginley and C. Bright, MRS Bull. **25**, 15 (2000).
2. B.J. Lewis and D.C. Paine, MRS Bull. **25**, 22 (2000).
3. K.L. Chopra, S. Major, and D.K. Pandya, Thin Solid Films **102**, 1 (1983).
4. S. Pizzini, N. Butta, D. Narducci, and M. Palladino, J. Electrochem. Soc. **136**, 1945 (1989).
5. D.M. Mattox, Thin Solid Films **204**, 25 (1991).
6. G. Phatak and R. Lal, Thin Solid Films **245**, 17 (1994).
7. A. Verkey and A.F. Fort, Thin Solid Films **239**, 211 (1994).
8. A.J. Freeman, K.R. Poeppelmeier, T.O. Mason, R.P.H. Chang, and T.J. Marks, MRS Bull. **25**, 45 (2000).
9. C.M. Cardile, A.J. Koplick, R. McPherson, and B.O. West, J. Mater. Sci. Lett. **8**, 370 (1989).

10. H. Kawazoe, M. Yasukawa, H. Hyodo, M. Kurita, H. Yanagi, and H. Hosono. Nature **389**, 939 (1997).
11. A.N. Banerjee, S. Kundoo, and K.K. Chattopadhyay, Thin Solid Films **440**, 5 (2003).
12. N. Duan, A.W. Sleight, M.K. Jayaraj, and J. Tate, Appl. Phys. Lett. **77**, 1325 (2000).
13. A. Kudo, H. Yanagi, H. Hosono, and H. Kawazoe, Appl. Phys. Lett. **73**, 220 (1998).
14. D.M. Mattox, Thin Solid Films **204**, 25 (1991).
15. K. Gurumurugan, D. Mangalaraj, and S.K. Narayandass, Thin Solid Films **251**, 7 (1994).
16. G. Sanatana, A.M. Acevedo, O. Vigil, F. Cruze, G. Contreras-Puente, and L. Vaillant, Superficiesy Vacio **9**, 300 (1999).
17. N. Ueda, H. Meada, H. Hosono, and H. Kawazoe, J. Appl. Phys. **84**, 6174 (1998).
18. M. Yan, M. Lane, C.R. Kannewurf, and R.P.H. Chang, Appl. Phys. Lett. **78**, 2342 (2001).
19. A.B.M.A. Ashrafi, H. Kumano, I. Suemune, Y.W. Ok, and TY. Seong, J. Crystal Growth **237–239**, 518 (2002).
20. S. Hayashi, Rev. Electr. Commun. Lab. **20**, 698 (1972).
21. K. Tanaka, A. Kunioka, and Y. Sakai, Jpn. J. Appl. Phys. **8**, 681 (1969).
22. P.K. Ghosh, R. Maity, and K.K. Chattopadhyay, Sol. Energy Mat. & Sol. Cells **81**, 279 (2004).
23. A. Elhichou, A. Bougrine, J.L. Bubendoref, J. Ebothe, M. Addou, and M. Troyon, Semicond. Sci. Technol. **17**, 607 (2002).
24. A.N. Banerjee, S. Kundoo, P. Saha, and K.K. Chattopadhyay, J. Sol-Gel Sci. Technol. **28**, 105 (2003).
25. JCPDS Powder Diffraction file card 5-0640.
26. M. Ito, H. Nagai, T.Tahata, S. Katsuyama, and K. Majima, J. Appl. Phys. **92**, 3217 (2002).
27. J.Y.W. Seto, J. Appl. Phys. **46**, 5247 (1975).
28. E. Shanthi, A. Banerjee, V. Dutta, and K.L. Chopra, J. Appl. Phys. **53**, 1615 (1982).
29. T. Pisarkiewicz, K. Zarkrzewska, and E. Keja, Thin Solid Films **174**, 217 (1989).
30. X. Wu, T.J. Coutts, and W.P. Mulligan, J. Vac. Sci. Technol. A **15**, 1057 (1997).
31. J.I. Pankove, in *Optical Processes in Semiconductors* (Prentice-Hall, Inc., New Jersey, 1971) p. 34.
32. K.K. Chattopadhyay, I. Sanyal, S. Chaudhuri, and A.K. Pal, Vacuum **42**, 915 (1991).
33. T.J. Cutts, D.L. Young, W.P. Mulligan, X. Li, X. Wu, and J. Vac. Sic. Technol. A **18**, 2646 (2000).
34. D.L. Young, T.J. Cutts, V.I. Kaydanov, A.S. Gilmore, and W.P. Mulligan, J. Vac. Sic. Technol. A **18**, 2978 (2000).